Breakdown of Functional Connectivity in Frontoparietal Networks Underlies Behavioral Deficits in Spatial Neglect

Biyu J. He,[1] Abraham Z. Snyder,[1,2] Justin L. Vincent,[1] Adrian Epstein,[1] Gordon L. Shulman,[2] and Maurizio Corbetta[1,2,3,*]
[1] Department of Radiology
[2] Department of Neurology
[3] Department of Anatomy and Neurobiology
Washington University School of Medicine, St. Louis, MO 63110, USA
*Correspondence: mau@npg.wustl.edu
DOI 10.1016/j.neuron.2007.02.013

SUMMARY

Spatial neglect is a syndrome following stroke manifesting attentional deficits in perceiving and responding to stimuli in the contralesional field. We examined brain network integrity in patients with neglect by measuring coherent fluctuations of fMRI signals (functional connectivity). Connectivity in two largely separate attention networks located in dorsal and ventral frontoparietal areas was assessed at both acute and chronic stages of recovery. Connectivity in the ventral network, part of which directly lesioned, was diffusely disrupted and showed no recovery. In the structurally intact dorsal network, interhemispheric connectivity in posterior parietal cortex was acutely disrupted but fully recovered. This acute disruption, and disrupted connectivity in specific pathways in the ventral network, strongly correlated with impaired attentional processing across subjects. Lastly, disconnection of the white matter tracts connecting frontal and parietal cortices was associated with more severe neglect and more disrupted functional connectivity. These findings support a network view in understanding neglect.

INTRODUCTION

Functional connectivity (FC) magnetic resonance imaging (MRI) studies temporal correlations between the blood oxygenation level-dependent (BOLD) signals in different brain regions. These temporal correlations are readily demonstrated in the resting state (i.e., in the absence of an explicit task; Biswal et al., 1995) and are contributed predominantly by low frequency (<0.1 Hz) fluctuations (Cordes et al., 2001). Coherent BOLD fluctuations within widely distributed but anatomically discrete networks recapitulate the spatial topography of task-evoked BOLD responses commonly observed with a variety of behavioral paradigms (e.g., somatosensory [Biswal et al., 1995], language [Hampson et al., 2002], default [Greicius et al., 2003; Laufs et al., 2003], and attention [Fox et al., 2005; Laufs et al., 2003]).

The behavioral significance of BOLD FC is poorly understood (but see Hampson et al. [2006a], [2006b] for two recent studies). One goal of the current study was to assess the behavioral significance of BOLD FC by measuring the relationship between FC and performance deficits in stroke patients longitudinally. The primary question was whether the degree of disruption in FC correlated with the severity of behavioral deficits at the acute stage and whether this correlation was maintained over the course of recovery.

A second goal of this study was to gain insights into the role of coherent BOLD fluctuations in the pathophysiology of neglect. Neglect is a common syndrome following right hemisphere strokes that includes both a rightward bias in spatial sensory-motor processing as well as several non-lateralized deficits of arousal, attentional capacity, and working memory (for reviews see Heilman et al. [1985]; Hillis [2006]; Husain and Rorden [2003]; Mesulam [1999]; Robertson [2001]). Neglect has been traditionally explained in terms of localized damage of specific brain structures (inferior parietal lobule [IPL; Mort et al., 2003; Vallar and Perani, 1987], superior temporal gyrus [STG; Karnath et al., 2001, 2004], subcortical nuclei [Karnath et al., 2002; Vallar and Perani, 1987], and the inferior frontal cortex [Husain and Kennard, 1996; Vallar and Perani, 1987]). The present work fits within a more recent perspective that emphasizes the importance of distributed dysfunction in frontoparietal cortical networks (Corbetta et al., 2005; Thiebaut de Schotten et al., 2005).

We have recently proposed that spatial neglect reflects dysfunction of two frontoparietal networks involved in the control of attention. The dorsal attention network controls the allocation of spatial attention to extrapersonal space and the selection of stimuli and responses predominantly

in contralateral space and includes as core regions the intraparietal sulcus (IPS) and the frontal eye field (FEF). The ventral attention network is necessary for target detection and reorienting toward salient unexpected events in either hemifield, is localized predominantly in the right hemisphere, and is centered around the temporoparietal junction (TPJ) and ventral frontal cortex (VFC; for review see Corbetta and Shulman [2002]). Strokes that cause neglect often structurally damage the ventral network while sparing the dorsal network (Corbetta et al., 2005; Husain and Rorden, 2003; Malhotra et al., 2006a; Milner and McIntosh, 2005). We have recently demonstrated, using a visuospatial attention task, that such strokes may lead to a functional imbalance of evoked responses in left (hyperactive) and right (hypoactive) dorsal parietal cortex, even though these areas are structurally intact (Corbetta et al., 2005). This imbalance correlates with the degree of contralesional inattention and recovers over time. These observations suggest that structural damage of the ventral network leads to functional impairment of the posterior parietal nodes of the dorsal network.

However, this previous fMRI study of neglect only examined task-evoked responses of individual regions. Inferences regarding network-level interactions were purely qualitative. Because stroke injury to part of a network may result in network dysfunction, direct assessments of functional interactions among brain areas using FC MRI should provide a better understanding of neglect. The dorsal and ventral attention networks were originally defined on the basis of task-evoked responses; more recently, using FC MRI acquired in healthy resting adults, Fox and colleagues (2006) showed that the same two networks emerge from an analysis of coherent spontaneous fluctuations of BOLD signals. Here, we measured interregional functional connectivity in these two attention networks in patients with neglect at both acute and chronic stages after the ictus. Performance measures on a visuospatial attention task were correlated with FC measures across subjects. The obtained results show that disrupted FC in the dorsal and ventral attention networks constitutes a critical mechanism underlying the pathophysiology of neglect.

RESULTS

Overview

To measure interregional FC, it was necessary first to identify regions of interest (ROIs) representing nodes in the dorsal and ventral attention systems. To this end, we reanalyzed data obtained in four previously published fMRI studies of visuospatial attention. Two sets of ROIs were defined and validated by FC mapping using data acquired in young healthy subjects, which showed that fluctuations were coherent within each system and largely independent across systems. Having defined two sets of functionally connected regions involved in attention-related functions, we measured interregional FC in patients and age-matched controls and determined whether

temporal correlations within fMRI signals correlated with behavioral performance across patients.

Normal Functional Connectivity of Dorsal and Ventral Attention Networks

ROIs in the dorsal and ventral attention networks were determined from a meta-analysis of four previously published event-related fMRI studies of young healthy adults in which spatial attention was manipulated using a Posner-like paradigm (Astafiev et al., 2003; Astafiev et al., 2004; Corbetta et al., 2000; Kincade et al., 2005; see Experimental Procedures and see Figure S1 in the Supplemental Data available with this article online). In each experiment the locus of attention was indicated on each trial by a central arrow pointing toward a left or right location on the computer screen. After a variable delay, a target appeared at either the cued location (75% of trials, "valid trials") or the opposite location (25% of trials, "invalid trials"). Subjects were instructed to maintain fixation on a central crosshair and to detect targets as quickly as possible. In different experiments, detection was signaled by a right-hand key press, a saccadic eye movement, a pointing hand movement, or object identification. Whole-brain ANOVA was conducted on each of the four studies (activation during cue period for dorsal attention regions, activation × validity during the period following target presentation for ventral attention regions) to identify significantly modulated voxels. The Z score maps were combined using a fixed-effects meta-analysis, and ROIs were then identified by an automated peak search algorithm.

Eight ROIs in the dorsal attention network (DAN) were consistently recruited in responses to the cue: bilateral FEF, posterior IPS (pIPS), ventral IPS (vIPS), and middle temporal area (MT$^+$; Figure 1A, yellow; Table S1, top). Several regions in the ventral attention network (VAN) were identified by consistently stronger activation to unexpected rather than expected targets: a precentral sulcus region (PrCe), middle frontal gyrus (MFG), anterior insula, TPJ, and superior temporal sulcus (STS; Figure 1A, orange; Table S1, bottom). All ventral regions were lateralized to the right hemisphere.

To confirm that these regions constitute separate FC networks, interregional temporal correlations of BOLD signals were examined in a data set of young healthy subjects (n = 12) performing the Posner task. Time courses were extracted from all regions in the right hemisphere, and the consistent task-evoked BOLD responses were removed by regression (see Experimental Procedures and Discussion). The interregional correlation matrix then was computed (Figure S2). Correlations between regions in different networks were significantly weaker than correlations between regions within the DAN (p < 0.0001) or within the VAN (p < 0.0003), indicating that the two networks are dissociable. To explore the distributed spatial topography of the correlated activity, seed ROI-driven FC maps were computed on a voxel-wise basis for each of the nine a priori attention regions in the right hemisphere. For each network, FC maps were combined using
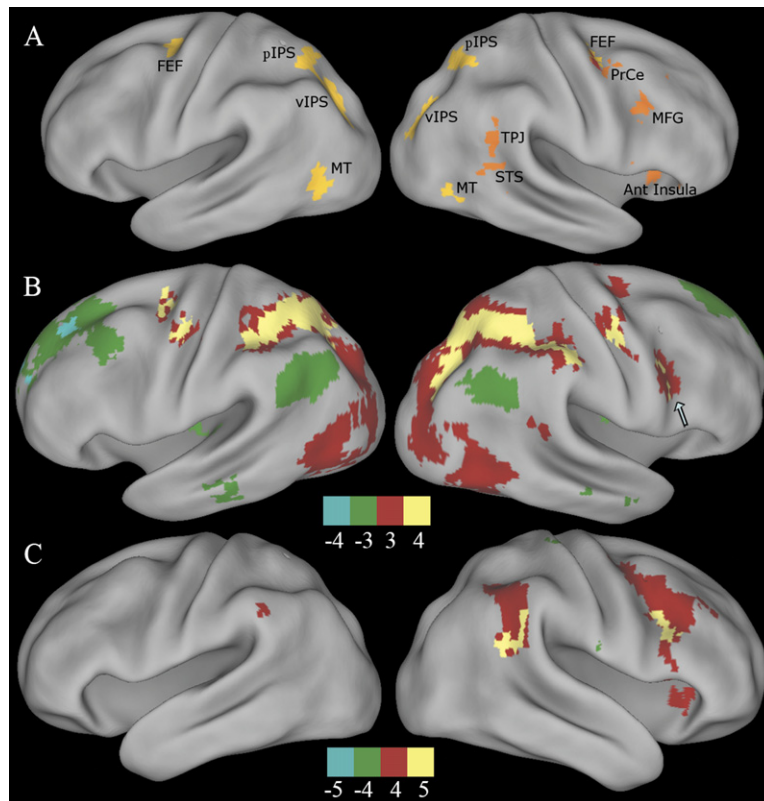
Figure 1. Dorsal and Ventral Attention Networks

(A) ROIs defined by activation fMRI studies and used as seed regions for FC analyses. Dorsal network regions, yellow; ventral network regions, orange. Region sizes were controlled to be about 900 mm^3.

(B) For each of the four right hemisphere DAN ROIs, group statistical maps were obtained using a random-effects analysis on the Fisher-transformed correlation maps and corrected for multiple comparisons at a significance level of p < 0.05 (z = 3, cluster size = 17 voxels). The four FC maps were combined to produce the conjunction map shown. Voxels in yellow are positively correlated with all four ROIs; red, positively correlated with three of four ROIs; green, negatively correlated with three of four ROIs; blue, negatively correlated with all four ROIs. Arrow points to the major right-lateralized region in the DAN, which overlaps with the VAN.

(C) FC maps from the five VAN ROIs were used to produce the conjunction map. Color code similar to (B).

a conjunction analysis that identified voxels correlated with at least three of four regions in the DAN (Figure 1B) or four of five regions in the VAN (Figure 1C). Although only right hemisphere regions were used as seeds, the FC-defined DAN network was largely bilaterally symmetric. Regions consistently correlated within the DAN included FEF, MT$^+$, and a large swath of cortex extending along IPS into extrastriate visual cortex. Consistent with task-activation studies, the FC-defined VAN network was strongly right lateralized and included the TPJ extending into the inferior parietal lobule, MFG, PrCe, and anterior insula. A small region also was detected in the left supramarginal gyrus (SMG). Interestingly, the largely bilateral DAN included a right-lateralized region in the middle and inferior frontal lobe (see arrow in Figure 1B), which overlapped with the VAN, suggesting this region may function as a link between networks (see also Fox et al. [2006]).

These two a priori sets of ROIs were then applied to the comparison of FC in patients versus in age-matched controls. Defining the ROIs in a separate group of young adults minimized the possibility of bias in the patient versus control comparison. The selected ROIs were complete in the sense that no other brain region outside the two networks showed robust attention-related BOLD response in patients at either stage (Figure S1).

Patients: Lesion Anatomy and Behavior

We longitudinally studied eleven patients with spatial neglect following right hemisphere stroke (mean age 59,

range 42–73, 2 female). Lesions were centered in the IPL, STG, frontal operculum, insula, as well as subcortical nuclei and white matter (Figure 2A). The distribution of lesions in this group is typical of larger samples (Karnath et al., 2004; Mort et al., 2003). All ROIs in the DAN were spared by the lesions, whereas ROIs in the VAN were damaged to various degrees. PrCe, MFG, TPJ, STS, and anterior insula were damaged in zero, two, four, three, and three patients, respectively (Figure 2A).

Patients performed the Posner task both in and out of the scanner at both the acute (30 ± 23 [mean ± SD] days poststroke) and the chronic (40 ± 11 weeks poststroke) stages of recovery. A group of twelve age-matched normal subjects (mean age 57.4, range 41–71, 7 female) were scanned while performing the Posner task in the same way as the patients.

Three types of behavioral deficits in the Posner task were assessed. A visual field (VF)-independent component of neglect was defined as increased misses and slowed reaction times (RT) across both visual fields as compared to controls. A VF-dependent component was defined as more misses and slower RTs in the contralesional than ipsilesional VF. Finally, a "disengagement deficit," common in neglect patients, was defined as specific impairment in detecting targets in the left VF following an invalid cue, as this condition requires disengaging attention from the good VF and reorienting to the bad VF (Friedrich et al., 1998; Morrow and Ratcliff, 1988; Posner et al., 1984).
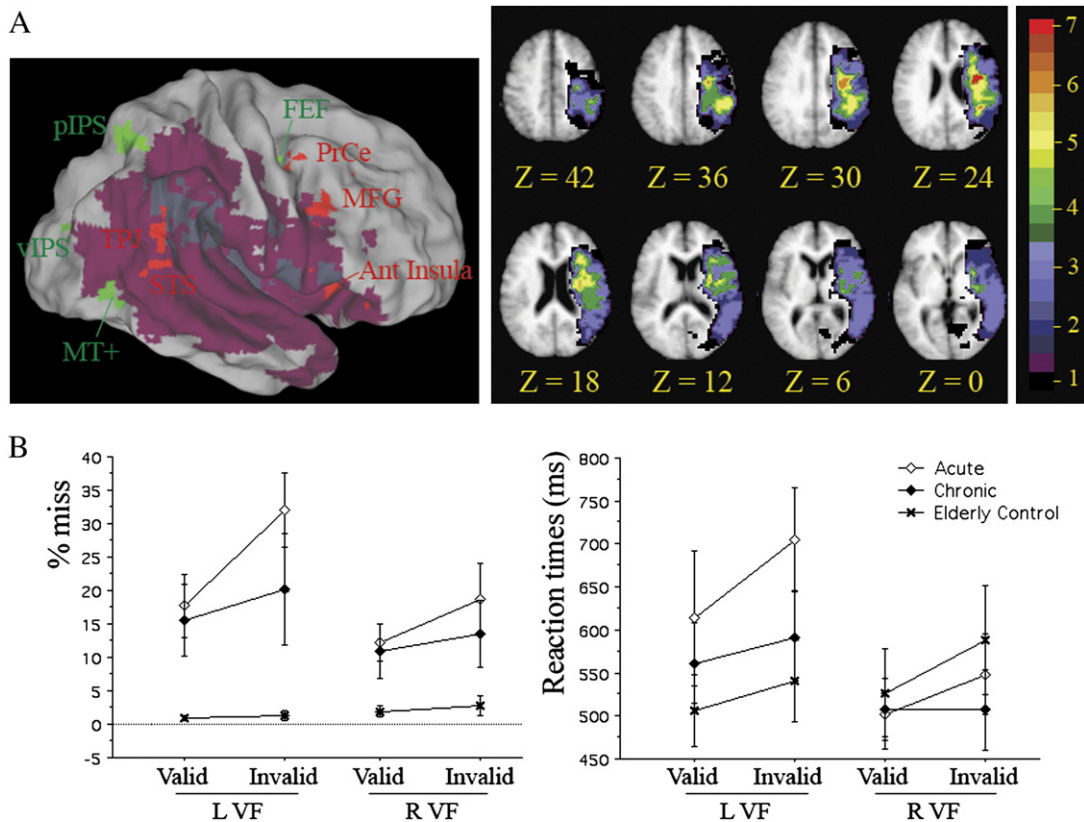
Figure 2. Lesion and Task Performance of Patients

(A) Left panel: group lesion anatomy (n = 11; purple, damaged in one to three patients; blue, damaged in four to seven patients) and ROIs constructed for FC analyses (DAN, green; VAN, red). Right panel: lesion overlap (n = 11) overlaid on patients' average anatomical image. Values denote the number of patients in which the particular voxel was damaged by lesion.

(B) Performance in the Posner task, compared with age-matched controls. Left, percent miss; right, RTs averaged across hit trials. Error bars denote SEM.

The behavioral performance of the patients was compared to age-matched controls using a three-way ANOVA, with group (control or patient), VF (left or right), and cue validity (valid or invalid) as factors (Figure 2B). Patients had significantly more misses than controls (VF-independent impairment, acute—$F_{1,22} = 19.5$, $p = 0.0002$; chronic—$F_{1,22} = 7.4$, $p = 0.01$), were particularly impaired in the left VF (lateralized impairment [VF × group], acute—hit rates, $F_{1,22} = 13.6$, $p = 0.001$; RT, $F_{1,22} = 17.8$, $p = 0.0004$; chronic—hit rates, $F_{1,22} = 2.45$, $p = 0.1$; RT, $F_{1,22} = 15.1$, $p = 0.0008$), and had a significantly greater disengagement deficit ([group × VF × validity], acute—hit rates, $F_{1,22} = 3.9$, $p = 0.06$; RT, n.s.; chronic—hit rates, n.s.; RT, $F_{1,22} = 4.27$, $p = 0.05$).

The improvement of behavioral performance from acute to chronic stage was not significant at the $p < 0.05$ level using the data from the scanner session, although the trends were in the expected direction (Figure 2B). A significant improvement was observed in separate acute and chronic sessions conducted in a regular testing room. Target detection improved overall in both visual fields ([stage], hit rates, $F_{1,9} = 5.6$, $p = 0.04$; RT, $F_{1,10} = 5.3$,

$p = 0.04$) and both rightward bias ([stage × VF], RT, $F_{1,10} = 6.4$, $p < 0.03$) and disengagement deficit ([stage × VF × validity], RT, $F_{1,10} = 8.3$, $p = 0.016$) were significantly reduced. Therefore, behavioral impairment including VF-independent, VF-dependent, and disengagement deficits recovered significantly over the interval between the acute and chronic sessions.

Functional Connectivity in DAN

We conducted several analyses to determine whether stroke affected basic characteristics of the BOLD signals, specifically, variance and temporal frequency distribution. These observations helped to rule out the possibility that the results presented below were artifact attributable to higher signal variance, more movement or abnormal neural-vascular coupling in patients (see Supplemental Data Note 1 and Figure S3 for methods and results).

We measured functional connectivity in the DAN after consistent task-related responses were removed from the time series (see Experimental Procedures and Discussion) and found a specific breakdown of FC between left and right pIPS. Left-right pIPS FC was reduced in acute
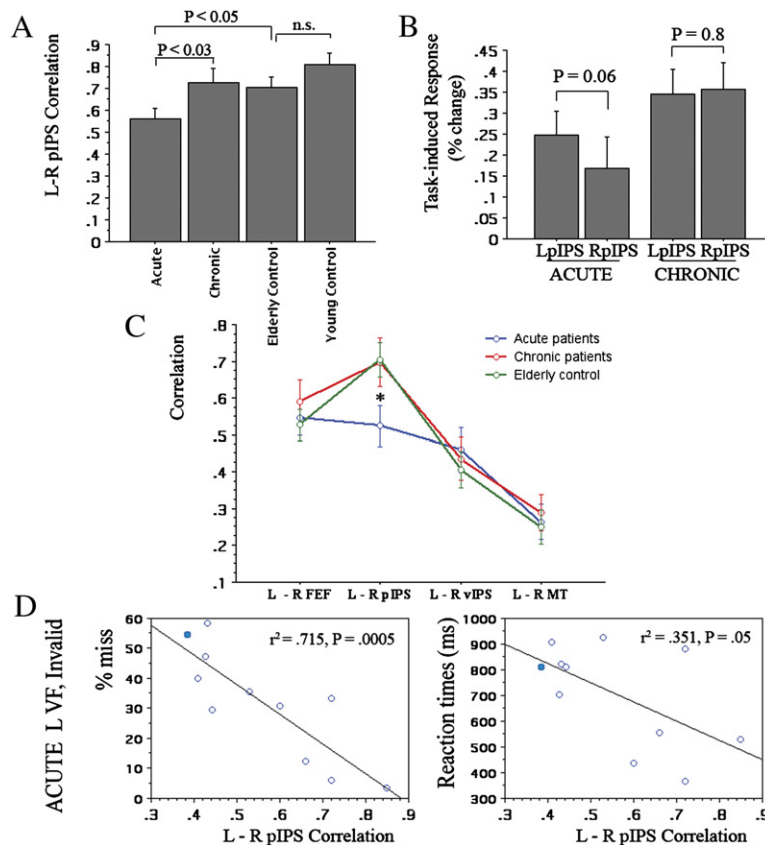
Figure 3. Left-Right pIPS FC

(A) Temporal correlation between left and right pIPS in patients (n = 11), elderly controls (n = 12), and young controls (n = 12).

(B) Rebalancing of task-evoked responses between left and right pIPS at chronic stage.

(C) Temporal correlations of all homologous pairs of regions in DAN, only left-right pIPS correlation was impaired acutely.

(D) Across acute patients, left-right pIPS FC significantly correlated with % miss (left panel) and RT (right panel) in detecting targets in the left VF following an invalid cue. Filled circle indicates the subject with largest lesion (200,928 mm^3). Error bars denote SEM.

patients as compared to age-matched controls (Figure 3A, p = 0.04, unpaired t test, two-tailed) but fully recovered at the chronic stage (Figure 3A; acute versus chronic, p < 0.03; chronic versus control, 0.72 ± 0.22 versus 0.70 ± 0.16). The disruption of interhemispheric FC was restricted to pIPS among the four homologous region pairs in the DAN (Figure 3C).

As noted above, we have previously shown an interhemispheric imbalance in task-evoked BOLD responses in dorsal posterior parietal cortex at the acute stage of neglect that recovers over time (Corbetta et al., 2005). This finding was reproduced in the current data set (with two subjects not included in the previous study): the right pIPS was less recruited than left pIPS at the acute stage, but the two sides showed balanced activation at the chronic stage (Figure 3B).

Critically, the breakdown of FC in dorsal parietal cortex was behaviorally significant. At the acute stage, there was a strong correlation between the strength of left-right pIPS FC and detection of targets in the left visual field following an invalid cue (Figure 3D, hit rates, r = 0.846, p = 0.0005; RT, r = −0.593, p = 0.05), such that the lower the interhemispheric FC in dorsal parietal cortex, the more impaired patients were in reorienting attention toward the neglected visual field. This correlation remained highly significant after correction for both lesion size and movement (hit rates, r = 0.699, p < 0.05). The data from the other

three trial types (left valid, right valid, right invalid) showed a similar trend that failed to reach significance (Table S2). The correlation between behavior and FC was specific to dorsal parietal cortex; no significant correlation with behavioral measures was found for the other three homologous region pairs in the DAN (for correlation with hit rates see Table S2).

Given that task-evoked responses are also abnormal in pIPS, an important question concerns whether the impairment of FC makes a difference beyond the abnormal evoked responses. Two analyses suggested that disrupted functional connectivity correlated with poor performance independently of task-evoked responses. First, there was no significant correlation between decreased FC and imbalanced task-evoked responses in pIPS (all p > 0.2, Table S3A). Second, partial correlation analyses demonstrated that controlling for the degree of abnormal task-evoked responses did not decrease and, in some cases, even slightly increased the FC-performance correlation (Table S3B).

At the chronic stage, the majority of patients showed improvement in both interhemispheric pIPS FC and performance, but three patients continued to show persistent impairments in both measures, resulting in a significant group correlation between these two measures (hit rates, left VF, valid—r = 0.619, p = 0.04; left VF, invalid—r = 0.587, p = 0.057; right VF, invalid—r = 0.712, p = 0.01).
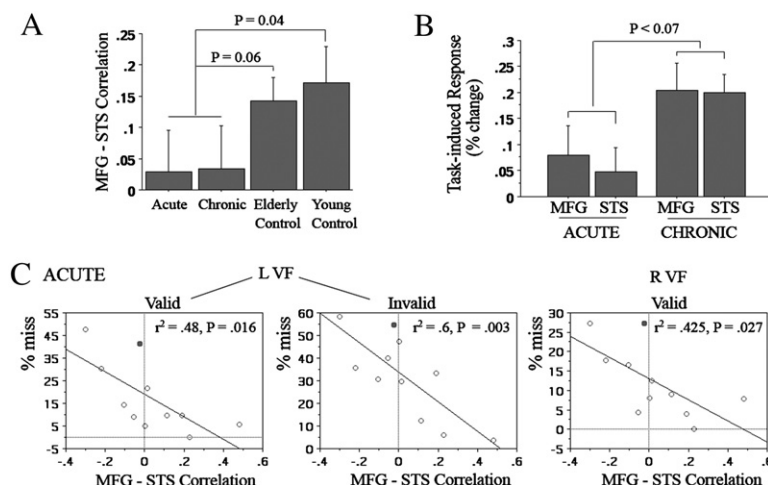
Figure 4. MFG-STS FC

(A) Temporal correlations between MFG and STS was significantly impaired in patients compared with controls and did not recover at the chronic stage. Error bars denote SEM.

(B) Task-evoked responses in MFG and STS.

(C) Across acute patients, MFG-STS FC significantly correlated with % miss in detecting targets in the left VF following valid (left panel) or invalid (middle panel) cues and in right VF following valid cues (right panel).

Behavioral relevance remained specific to interhemispheric pIPS FC; neither vIPS, FEF, nor MT FC showed correlation with performance (either hit rates or RTs).

Functional Connectivity in Visual Cortex

Consistent with models of attention that posit feedback interactions from attention-controlling dorsal parietal regions to data-processing visual regions (Corbetta and Shulman, 2002; Kastner and Ungerleider, 2000), an imbalance of task-evoked activity similar to that demonstrated in dorsal parietal cortex has been recorded in visual cortex in patients with left neglect (Corbetta et al., 2005). Accordingly, we measured temporal correlations between left and right visual cortex, using ROIs in retinotopic occipital cortex defined by functional and anatomical criteria (as in Corbetta et al. [2005]). Interestingly, interhemispheric FC in visual cortex was completely intact (acute versus chronic versus age-matched controls—dorsal retinotopic ROIs, 0.77 ± 0.07 versus 0.77 ± 0.07 versus 0.78 ± 0.07; ventral retinotopic ROIs, 0.74 ± 0.10 versus 0.72 ± 0.16 versus 0.69 ± 0.07). Thus, an interhemispheric imbalance in task-evoked activity was not necessarily accompanied by a breakdown of interhemispheric FC, indicating that abnormal task-evoked activity does not lead to abnormal FC. The observation of intact FC in visual cortex but disrupted FC in dorsal parietal cortex, however, does not contradict the presence of top-down modulation, which might be more dynamic and task-dependent, i.e., manifesting within task-induced responses. Neither task-evoked responses (Corbetta et al., 2005) nor FC in visual cortex correlated with behavioral performance, indicating that spatial neglect is less related to the functioning of visual cortex than to parietal cortex.

Functional Connectivity in VAN

The structural integrity of regions in the VAN and, presumably, of their respective anatomical connections, was compromised by stroke to different degrees in different patients. Correspondingly, we found a global impairment of functional connectivity in the ventral network, which

did not recover (see Figure 4A for MFG-STS FC, see Figure S4 for all pairwise FC within the VAN).

Behavioral correlations with FC at the acute stage were largely restricted to MFG-STS and MFG-TPJ (Table S2). MFG-STS FC correlated significantly with hit rates in both visual fields in the valid condition (left VF, r = 0.693, p = 0.016; right VF, r = 0.652, p = 0.027) and in the left visual field, invalid condition (r = 0.775, p = 0.003; Figure 4C). MFG-TPJ FC correlated with hit rates only in the valid conditions, but again in both visual fields (L VF, r = 0.747, p = 0.006; R VF, r = 0.731, p = 0.008, data not shown). Results after correction for both movement and lesion size are shown in Table S3.

Interestingly, the task-evoked responses in these areas did show some evidence of recovery (e.g., Figure 4B, p = 0.067), indicating that these regions might have independently partially regained function.

So far we have assessed all pairwise FC between the five a priori ROIs in the VAN. Since the VAN as defined by FC also included a left SMG region (see Figure 1C), we assessed the FC between this L SMG region and its homologous right hemisphere region (R SMG). (This L SMG region showed a significant validity × time effect in the meta-analysis of young adult fMRI [Figure S1B] but did not pass the threshold used in the peak-search algorithm and therefore was not included in the a priori set of ROIs.) First, voxel-wise FC maps obtained by seeding the L SMG (Figure S5A) and R SMG (Figure S5B) confirmed the right hemisphere laterality of the VAN. The interhemispheric SMG FC, as most of other pairwise FC in the VAN (Figure S4), was acutely disrupted and did not recover (Figure 5A). Task-evoked responses in SMG were similar to those in pIPS in the sense that an acute imbalance recovered at the chronic stage, although these effects did not reach statistical significance (Figure 5B). Interhemispheric FC of the SMG significantly and specifically correlated with disengagement deficit at the acute stage (Figure 5C, with % miss, p < 0.001, significant after correction for both movement and lesion size [Table S4]; with RT, p = 0.03). In this characteristic the SMG was
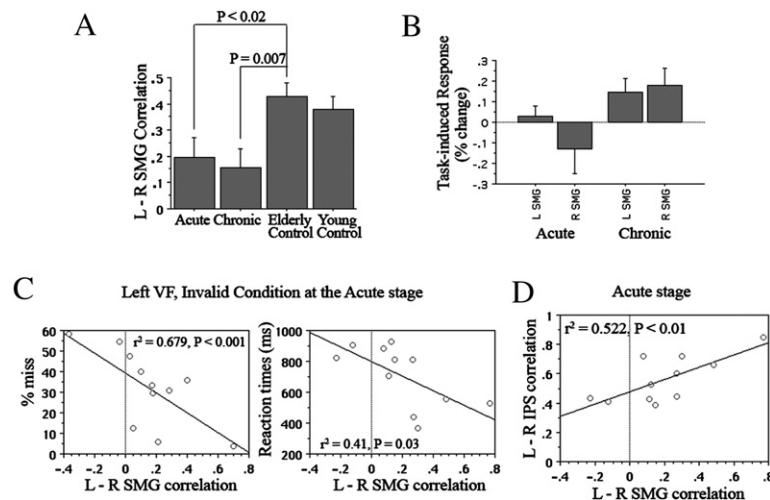
Figure 5. Left-Right SMG FC

(A) Temporal correlation between left and right SMG was significantly impaired in patients compared with controls and did not recover at the chronic stage. Error bars denote SEM.

(B) Task-evoked responses in left and right SMG.

(C) Across acute patients, L-R SMG FC significantly correlated with % miss (left) and RT (right) in detecting targets in the left VF following an invalid cue.

(D) Across acute patients, interhemispheric FC in pIPS and in SMG correlate with each other.

also similar to the pIPS. Moreover, there was a significant positive correlation between decreased pIPS FC and decreased SMG FC (Figure 5D). However, unlike interhemispheric pIPS FC, interhemispheric SMG FC showed no recovery from acute to chronic stages.

Interaction between DAN and VAN

The results presented up to this point indicate that strokes associated with spatial neglect cause an acute disruption of FC between left and right dorsal parietal cortex, persistent breakdown of FC between several regions of the VAN, and robust correlation of disrupted FC with impaired performance in a spatial attention task. Below, we consider whether spatial neglect was associated with a deficit in the interaction between pIPS and the VAN.

First, we found that the physiological impairments in the two networks were highly correlated. Decreased MFG-STS FC (Figure 6A, r = 0.781, p = 0.003) and decreased interhemispheric SMG FC (Figure 5D, r = 0.722, p < 0.01) each significantly correlated with decreased interhemispheric pIPS FC at the acute stage. Although this correlation might result from intersubject variability in fMRI signal quality, FC of no other pair of regions within the VAN correlated with left-right pIPS FC, strongly arguing against this possibility. These correlations between pIPS FC and VAN FC were not observed in either the young or old control groups, suggesting this relationship was specific to the pathophysiology in patients.

Second, we investigated the anatomical basis of spatial neglect and its relation to disrupted FC. We divided the patients into two subgroups (each n = 5) based on a median-split of the severity of left sided neglect at the acute stage (calculated as % miss and RT [left-right VF], averaged across valid and invalid trials). The two subgroups significantly differed at the acute stage in leftward neglect (VF × group—hit rates, $F_{1,8}$ = 20.7, p < 0.002; RT, $F_{1,8}$ = 35.1, p = 0.0004) and in overall detection speed across both visual fields (RT, $F_{1,8}$ = 8.14, p = 0.02; Figure 7A). Moreover, consistent with results presented earlier, at the acute stage, interhemispheric pIPS FC (p < 0.04), MFG-STS FC (p < 0.07), and interhemispheric SMG FC (p < 0.01), but not MFG-TPJ FC (p = 0.89), were all lower in patients with more severe neglect (Figure 7C). When we contrasted voxel-wise the distributions of anatomical damage in the two groups, we discovered that a region located at the arcuate fasciculus (AF) and the superior longitudinal fasciculus (SLF) was damaged in all patients with more severe neglect but was spared in all patients with milder neglect (Figure 7B). The AF connects middle frontal areas with superior temporal areas (Petrides and Pandya, 2002), providing a possible structural basis for the disruption of MFG-STS FC. Since part of MFG is temporally correlated with both networks (Figure 6B), interruption of the MFG-STS connectivity might also affect communication between the VAN and pIPS. The SLF connects both the superior and inferior
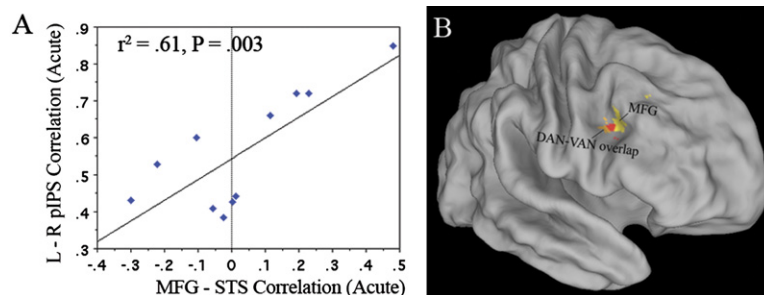

Figure 6. MFG as a Potential Link between DAN and VAN

(A) Correlation between MFG-STS FC and left-right pIPS FC across acute patients.

(B) Part of MFG ROI is temporally correlated with both networks. MFG ROI used in FC analyses (yellow) and the overlap region (orange) between DAN (thresholded as 3/4) and VAN (thresholded as 4/5). Overlap between MFG ROI and the DAN-VAN overlap region is shown in red.
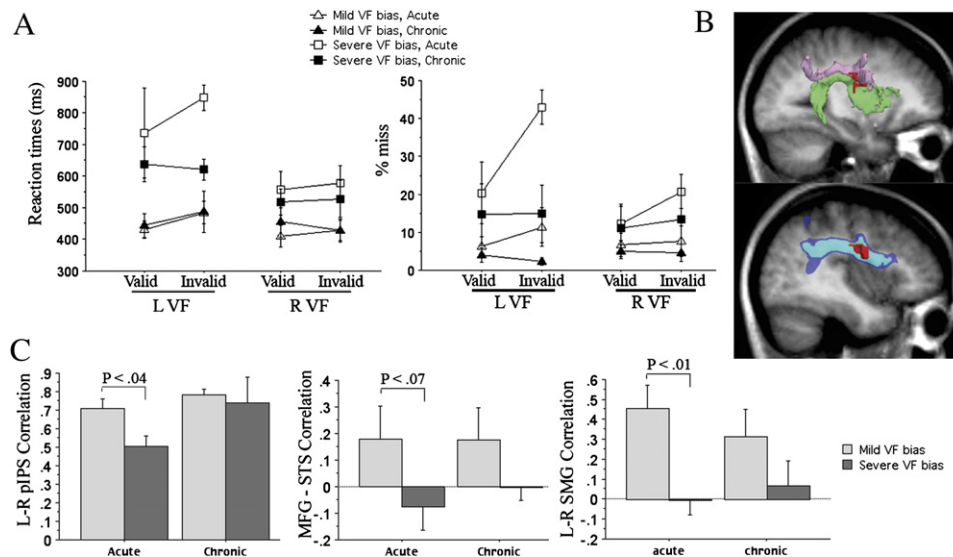
Figure 7. Median Split of All Patients Based on VF Bias at the Acute Stage

(A) Behavioral performance of each subgroup at acute and chronic stages.

(B) A white matter region (red) was damaged in all patients from the severe subgroup but spared in all patients from the mild subgroup. Top: streamline diffusion tensor tractography (sDTT) of the superior longitudinal fasciculus (SLF, pink) and the arcuate fasciculus (AF, green), with the lesion spot shown in red. The relatively abrupt anterior ending of the SLF was likely due to the crossing corticospinal tracts. Bottom: probabilistic DTT seeded in the lesion (red). Voxels in which >5% of all tracts from the seed pass through are shown in dark blue. Voxels in which >10% of tracts from the seed pass through are shown in light blue.

(C) The subgroup with severe VF bias also had more impaired left-right pIPS FC, MFG-STS FC and left-right SMG FC.

parietal lobules with dorsolateral prefrontal cortex (Schmahmann and Pandya, 2006), providing a plausible structural basis for the disruption of frontoparietal FC in the VAN. More importantly, disrupted SLF may also damage the communication between ventral frontal component of the VAN and posterior parietal component of the DAN. Supporting this hypothesis, FC between MFG and pIPS was strongly disrupted and did not recover (Figure S4).

Finally, results from a single case not included in the previous analyses indicated that disrupted interhemispheric pIPS FC alone does not lead to severe neglect. This patient (age 36) suffered a right dorsal medial parietal lesion that extended into the corpus callosum and presumably partially damaged the fibers connecting left and right posterior parietal cortices (Figure 8A). As might be predicted, interhemispheric FC in pIPS was 2.8 standard deviations (SD) lower than the mean of the whole group at the acute stage (1.5 SD lower at chronic stage; Figure 8B, left). However, this patient had a very mild VF bias (Figure 8B, middle and right, ~1 SD below the mean of the patient group and not significantly different from controls). Therefore, our data suggest that decreased pIPS interhemispheric BOLD FC alone is not sufficient to cause severe neglect. In other words, it appears that the severity of left neglect robustly correlates with decreased interhemispheric pIPS FC only in the presence of a damaged VAN. This clinical case, together with similar previous observations (e.g., Quigley et al. [2003]), sup-

ports a view that corticocortical connections provide a structural basis of BOLD functional connectivity.

DISCUSSION

We have demonstrated the behavioral significance of BOLD functional connectivity by showing an across-subject correlation of disrupted FC and the severity of spatial neglect. The results also suggest that disrupted functional connectivity in the two attention networks underlies different components of the syndrome and yet correlate with each other. These findings emphasize a network view of neglect and, more generally, stroke. Below, we discuss how these results enhance our understanding of the neural basis of spatial neglect and support the use of FC MRI as a clinical tool.

Understanding Spatial Neglect with Connectivity in Mind

We have proposed that it is the conjunction of structural and functional damage to the ventral and dorsal frontoparietal attention networks that causes neglect. This view explains why neglect patients usually show both spatially lateralized (i.e., neglect of contralesional space) and nonlateralized (i.e., low arousal, impaired working memory, lower attentional capacity) deficits. Previous studies in healthy subjects indicate that the dorsal network mediates control of spatial attention with a contralateral bias (Corbetta et al., 2002; Macaluso et al., 2002; Sereno
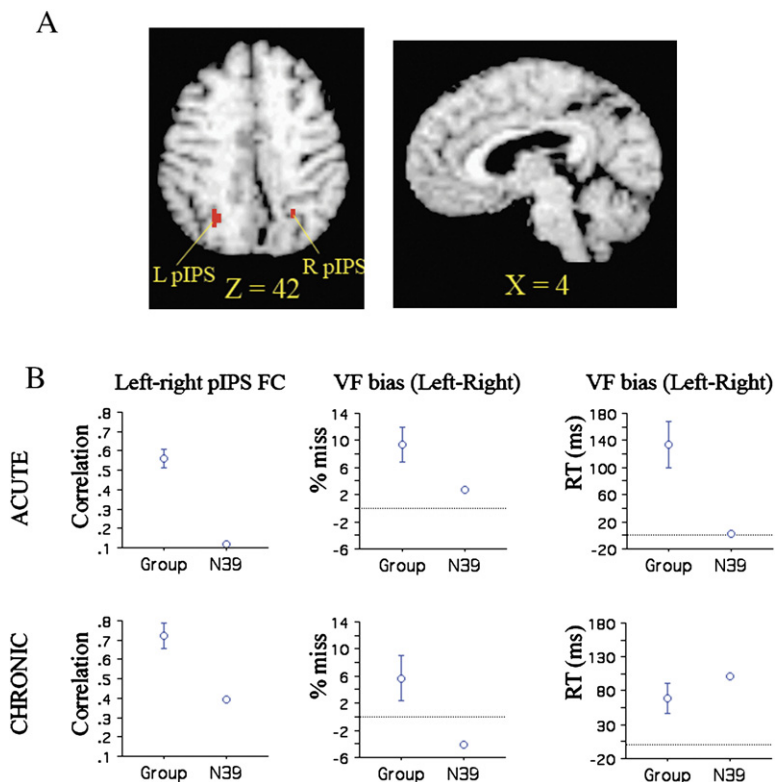
Figure 8. Single Case with Right Dorsal Medial Parietal Lesion

(A) pIPS ROI (red) overlaid on patient's own anatomical image.

(B) Comparison of the single case (N39) to the mean of all the other patients (n = 11). Left, interhemispheric pIPS FC. Middle (% miss) and Right (RT), measurements of rightward visual field bias (% miss and RT) evaluated as (left VF) − (right VF), collapsed across valid and invalid trials. Error bars denote SEM.

et al., 2001; Silver et al., 2005), while the ventral system is involved in nonlateralized attentional functions, including spatial and temporal capacity (Husain and Rorden, 2003; Peers et al., 2005; Shapiro et al., 2002) vigilance (Pardo et al., 1991; Rueckert and Grafman, 1996; Wilkins et al., 1987), saliency detection (Downar et al., 2000; Serences et al., 2004), and reorienting of attention (Arrington et al., 2000; Corbetta et al., 2000; Macaluso et al., 2002). According to this account, structural damage to the right hemisphere ventral regions, which is the most commonly lesioned area in spatial neglect, causes nonlateralized deficits directly and lateralized deficits indirectly, through distant effects on the dorsal parietal cortex that induce functional abnormalities therein.

This general framework is well supported by the current results. The pIPS was the only region in the dorsal network showing (at the acute stage) both a breakdown of interhemispheric FC and an imbalance (left > right) of task-evoked responses. Critically, both abnormalities were associated with impaired behavioral performance, especially detection and reorienting in the left VF, and both abnormalities recovered completely at the chronic stage. The pIPS region normally is recruited by allocation of attention covertly or overtly (Corbetta et al., 1998), is adjacent to regions involved in planning arm movements (Astafiev et al., 2003), and contains a complete representation of the contralateral visual field (Schluppeck et al., 2005; Silver et al., 2005). It is therefore well positioned to mediate spatially lateralized deficits of neglect that typically involve attention, perception, and responding. Consistently, inter-

hemispheric pIPS FC most strongly correlated with the disengagement deficit, which reflects the lateralized component of neglect (i.e., left hemi-inattention).

In the VAN, significant correlations between MFG-TPJ FC and behavioral deficits were the same in both visual fields, consistent with the hypothesized contribution of the VAN to the nonlateralized component of neglect. Interestingly, MFG-STS FC showed a similar, albeit weaker, behavioral correlation pattern as interhemispheric pIPS FC, suggesting that TPJ and STS, although both part of the ventral network, may have distinct attentional functions. Another interesting result was that the degree of interhemispheric SMG FC closely correlated with the disengagement deficit in the left visual field, a correlation similar to that observed for left/right pIPS. This result may suggest that, at the acute stage, successful reorienting to unattended targets requires interhemispheric coordination between ventral parietal areas involved in detecting unattended targets (Astafiev et al., 2006; Corbetta et al., 2000; Macaluso et al., 2002) and dorsal parietal areas involved in shifts of attention. However, at the chronic stage, an improvement in the disengagement deficit was accompanied with a recovery of interhemispheric FC in dorsal parietal but not ventral parietal cortex.

While these results suggest some dissociation of the neural systems underlying lateralized and nonlateralized deficits, to the extent that greater VAN damage causes greater disruption in pIPS FC, lateralized and nonlateralized deficits should be correlated. Indeed, multiple studies have indicated an interaction between these two

components of neglect (Robertson, 2001; Robertson et al., 1998), consistent with the strong correlation between lateralized (e.g., difference between left and right VFs) and nonlateralized (e.g., averaged across VFs) behavioral deficits observed here (RT, r = 0.68, p = 0.01). Clinical interventions that enhance nonspatial vigilance improve leftward spatial neglect (Malhotra et al., 2006b; Robertson et al., 1995, 1998), again suggesting a functional interaction between ventral and dorsal attention networks.

What is the functional-anatomical locus of this interaction? The close association between ventral structural damage and pIPS functional abnormalities suggests that pIPS is the major component of the dorsal network receiving input from the ventral network. Several converging results suggest that this input might come from right MFG. First, in the intact brain, right MFG shows BOLD signal temporal correlations with both VAN and DAN (Figure 6B), suggesting it may function as a node shared between the two networks. Second, MFG-pIPS FC was as strong as within-VAN FC in elderly controls but was severely and persistently disrupted in patients. In concert, the median-split lesion analyses indicated that patients with more severe spatial neglect sustained damage of the SLF, which connects dorsolateral prefrontal cortex to superior and inferior parietal lobules, providing a plausible structural basis for the disruption of MFG-pIPS FC and MFG-TPJ FC. Third, disrupted FC between left and right dorsal parietal cortex was positively correlated with disrupted FC between STS and MFG. Fourth, behaviorally significant FC within the right hemisphere ventral network almost always involved the MFG. More speculatively, there is evidence that stimulation of a tract that could plausibly connect MFG to the posterior parietal cortex produces neglect-like symptoms (Thiebaut de Schotten et al., 2005). Furthermore, lesions causing neglect in both monkeys and humans tend to involve intrahemispheric white matter long-range tracts bidirectionally connecting parietal and frontal cortices (Gaffan and Hornak, 1997; Bartolomeo et al., 2007).

Slightly complicating this picture, recovery of pIPS FC and task-evoked responses depended neither on the recovery of FC in the ventral network nor on the recovery of FC between MFG and pIPS. Speculatively, recovery of dorsal parietal cortex function, paralleling behavioral recovery, may reflect a stronger volitional control of the locus of spatial attention that results from the clinical rehabilitation and treatment of neglect patients (Diller and Weinberg, 1977).

Lastly, we revisit the long-standing puzzle that neglect is more frequent, severe, and enduring following right than left hemisphere lesions. Traditionally, theories of neglect have proposed that the lateralization of neglect reflects an asymmetrical representation of space in the two hemispheres (Heilman and Van Den Abell, 1980; Hillis, 2006; Mesulam, 1999). In the current view, spatial representations are contained in the DAN, which is bilaterally symmetric. It is the VAN, which encodes nonspatial func-

tions, that is strongly lateralized to the right hemisphere, as suggested by task-activation (summarized in Corbetta and Shulman [2002]) and FC (Fox et al. [2006] and the present results) studies. Even when a left SMG region was selected as seed ROI, we found a lateralization to the right hemisphere of the ventral frontoparietal FC (Figure S5). Therefore, right hemisphere strokes are more likely to damage the VAN, and through its connections with the DAN via intrahemispheric white matter tracts, more likely to cause a significant functional imbalance in posterior parietal cortex that will secondarily cause a rightward bias with left field detection deficits. Furthermore, nonspatial functions mediated by the VAN will be more permanently damaged after a right hemisphere stroke. Our model suggests that the right lateralization of strokes causing neglect reflects primarily a lateralization of nonspatial functions rather than spatial functions, which when disrupted also produce asymmetrical deficits in spatial functions.

Dissociation of FC and Task-Activation Measures

Our data suggest that abnormal task-evoked responses and functional connectivity represent different and complementary physiological indicators of dysfunction. Table S3 shows that the correlations between FC and performance were independent of task-evoked responses. Moreover, impairments in these two measurements could occur independently: imbalanced interhemispheric task-evoked responses occurred in the presence (e.g., pIPS) or absence (e.g., visual cortex) of disrupted FC; recovery of task-evoked responses in two regions was accompanied (e.g., left-right pIPS) or not accompanied (e.g., MFG-STS) by recovery of functional connectivity. At this stage, we note that a thorough understanding of these dissociations will need further experimental work.

FC MRI of Resting-State Data versus Task-State Data

It is important to note that our FC analyses were conducted on fMRI data that were acquired while subjects performed an event-related attention task rather than at rest, but with the deterministic (i.e., consistent) task-evoked effects removed. For a detailed discussion on the potential difference between FC results using the current method and those using resting-state data see Supplemental Data Note 3.

Functional Connectivity versus Anatomical Connectivity

The current work is also relevant to understanding the relation of functional connectivity to anatomical connectivity. BOLD functional connectivity produces networks with spatial patterns similar to those of anatomical connectivity (for discussion, see Vincent et al. [2006]), i.e., coherent BOLD relationships appear to depend on anatomical connectivity. However, functional connectivity between regions can be disrupted in the absence of anatomical damage to those regions or their connections

(e.g., interhemispheric pIPS FC in all the 11 patients), suggesting that anatomical connectivity may be necessary but not sufficient for normal functional connectivity; excitatory/inhibitory neuronal inputs from other regions are also needed.

FC MRI as a Tool for Studying Patient Populations

FC MRI is a promising new tool for the investigation of brain-behavior relationships in patient populations. It makes no demands on the subject other than holding still and possibly maintaining fixation and therefore can be acquired even in patients that cannot perform a task (for some examples of resting-state FC studies in patients, see Greicius et al., [2004]; Lowe et al. [2002]; Quigley et al. [2001]; Waites et al. [2006]); for a study using similar approach as the current study see Whalley et al. [2005]). This significantly widens the range of patients that can participate in functional brain-imaging protocols. Moreover, FC measures are less confounded by differences in task performance between patient and control groups or between patient groups at different stages of recovery, as compared to conventional task-activation measures. This is particularly true for resting-state FC MRI. Finally, FC MRI is robust and reliable in individual subjects after relatively short (5–15 min) scanning sessions and is therefore suitable to clinical applications.

Previous studies of FC in patient populations have usually described group differences in the spatial pattern or strength of FC between patients and controls. Our study, which shows that across subjects the disruption of FC indexes the severity of impaired performance, (see Hampson et al. [2006a, 2006b]) for similar correlations in healthy subjects), provides stronger evidence that intact BOLD FC is critical for normal brain function.

EXPERIMENTAL PROCEDURES

Subjects

Eleven patients (two female), mean age 59 years, with right frontoparietal stroke and initially demonstrated neglect participated in the study. All provided informed consent according to procedures established by the Washington University Institutional Review Board. All patients underwent standard rehabilitation for at least 3 months after the stroke. Patients were tested twice: once in the acute stage, i.e., ∼4 weeks (mean 30 days) after the stroke, and once at the chronic stage, i.e., more than 6 months (mean 40 weeks) after the ictus. Inclusion criteria were as follows: (1) age 18 or greater, no upper age limit applied; (2) single right hemisphere lesion, ischemic or hemorrhagic; (3) clinical evidence of neglect on clinical screening; (4) awake, alert, and capable of understanding and participating in research; (5) able to tolerate the scanner environment for 2 hr within the first 4 weeks after the stroke. Exclusion criteria were as follows: (1) evidence by CT or MRI of other strokes, although up to two lacunes were allowed in the subcortical white matter; (2) inability to maintain wakefulness; (3) presence of other neurological, psychiatric, or medical conditions precluding active participation in research or altering the interpretation of behavioral/imaging studies (e.g., dementia, schizophrenia), or limited life expectancy to less than 1 year (e.g., cancer or congestive heart failure class IV); (4) carotid stenosis greater than 50% by Doppler studies or angiogram (as the BOLD response in the hemisphere ipsilateral to a carotid stenosis may not reliably track neuronal activity); (5) claustrophobia.

Twelve young (six female; age 18–38 years) and twelve older (seven female; mean age 57.4, range 41–71) healthy subjects were recruited from the Washington University community to serve as control subjects. All control subjects were right-handed and had no neurological history. All gave informed consent following guidelines set by the WU Institutional Research Board and were compensated for their time.

Apparatus and Stimuli

Stimuli were generated by an Apple Power Macintosh computer and projected onto a screen at the head of the magnet bore by a Sharp LCD projector. Participants viewed the stimuli through a mirror attached to the head coil. Stimuli were white on a black background.

Task

The Posner task was implemented as follows in patients and elderly controls: the display contained two boxes (unfilled squares) each 1° on a side, centered 3.3° to the right and to the left of the central fixation point. Each trial started with the fixation point changing color from red to green. After 800 ms, an arrow cue pointing left or right was presented at the fixation locus for 2360 ms. Following a delay ranging from 1500 to 3000 ms, an asterisk target was presented for 100 ms in one of the two boxes. Left and right targets were equally probable. On 75% of the trials, the target was presented at the location indicated by the cue (valid), while on 25% of the trials, it was presented at the opposite location (invalid). The subject indicated target detection as quickly as possible with a right hand key press. Reactions times (RTs) were measured in milliseconds from the appearance of the target to the key press. The next trial began after an intertrial interval (ITI) that was randomized between 4760 and 9440 ms. The standard session involved eight fMRI runs of 5 min each, where each run contained about 20 trials. At the acute stage, we obtained between 6 and 12 fMRI runs (mean = 8.9) per subject. At the chronic stage, the number of fMRI runs ranged from 7 to 12 (mean = 9.6). Eight fMRI runs were obtained in each elderly control subject.

The Posner task procedure for young controls differed slightly: (1) 20% of trials ended immediately after the cue; in another 20% of trials, the cue was followed by a test period lasting 4.72 s in which no target was presented; (2) the cue-target interval varied between 3860 and 5360 ms; (3) the ITI lasted for two, three, or four frames. The number of fMRI runs ranged from 11 to 16 (mean 15.1).

fMRI Scan Acquisition

Scanning was performed with a Siemens 1.5 T Vision MRI scanner. Functional data were acquired using an asymmetric spin-echo, echo-planar imaging sequence sensitive to BOLD contrast (TE = 37 ms, TR = 2.36 s, flip angle = 90°; 16 contiguous 8 mm slices with 3.75 × 3.75mm in-plane resolution). The functional data slice tilts and field of view were prescribed parallel to the AC-PC plane on the basis of a short (<2 min) prefunctional coarse MP-RAGE scan. Each fMRI run included 128 frames (volumes). Compensation for asynchronous (interleaved) slice acquisition was accomplished by sinc interpolation. The functional data were realigned within and across fMRI runs to correct for head motion. Each fMRI run was intensity scaled to yield a whole-brain mode value of 1000 (not counting the first four frames). Anatomical images were acquired using a sagittal MP-RAGE sequence (TR = 97 ms, TE = 4 ms, flip angle = 12°, inversion time = 300 ms). For each subject, an atlas transformation to the atlas representative template was computed on the basis of an average of the first frame of each fMRI run and MP-RAGE structural images. Our template was produced by mutual coregistration of images obtained in 12 normal subjects and represents the Talairach coordinate system (Talairach and Tournoux, 1988). Each fMRI scan was interpolated to 3 mm cubic voxels in atlas space. Time series were combined within each session, and event-related responses were extracted using the general linear model, making no assumptions regarding the hemodynamic response shape. Regional time courses were extracted by averaging within the regions. Magnitudes were computed as the inner product of the time courses

with a canonical hemodynamic response function of the γ type (Boynton et al., 1996).

Anatomical Imaging and Lesion Segmentation

Multiple anatomical images were acquired using a sagittal T1-weighted MP-RAGE sequence (TR = 97 ms, TE = 4 ms, flip angle = 12°, inversion time = 300 ms, 1 × 1 × 1.25 mm voxels) and a T2-weighted fast spin echo sequence. All anatomical data acquired in each subject were spatially mutually coregistered and resampled in atlas space to 1 mm³ voxels. Atlas registration error attributable to the presence of a lesion was measured by computing the transformation with and without excluding the lesion and determined to be less than 2 mm for the largest lesion in this group of patients. The coregistered MP-RAGE images were averaged to increase the contrast to noise ratio. Artifactual intensity in homogeneity was corrected using a 3D parabolic (ten free parameters) model of the gain field. Lesion boundaries were determined with the aid of an unsupervised bispectral (T1-weighted plus T2-weighted) fuzzy class means (FCM) procedure that classified voxels into one of four categories: air, cerebrospinal fluid (CSF), gray matter, and white matter. Expert judgment was required to correctly segment the lesion on the basis of the automatic classification, e.g., to distinguish CSF representing a cystic lesion versus lateral ventricle.

Functional Connectivity Analyses
Additional Preprocessing

In preparation for FC analysis, the BOLD volumetric time series were passed through several additional preprocessing steps: (1) spatial smoothing using a 6 mm full width at half maximum Gaussian blur; (2) temporal filtering retaining frequencies in the 0.009–0.08 Hz band; (3) removal by regression of several sources of variance unlikely to reflect spatially-specific functional correlations—(i) six parameters obtained by correction of head motion, (ii) the signal averaged over the whole brain (excluding the ventricles and, in patients, the stroke lesion), (iii) the signal from a ventricular region, (iv) the signal from a white matter region. Temporal derivatives of these regressors were included in the linear model, thereby accounting for the time-shifted versions of spurious variance (e.g., delayed whole brain BOLD signal in venous structures). Deterministic task-evoked response components were removed by including, for each distinct trial type (left-valid, left-invalid, right-valid, right-invalid), eight regressors corresponding to frames 0 through 7 following the trial onset (cue presentation; for an evaluation of the efficacy of this maneuver see Supplemental Data Note 2). Trials of varying cue-target interval were lumped together as the difference between the shortest and longest interval (1.5 s) was less than one frame TR (2.36 s). The total number of regressors used to remove spurious sources of variance as well as deterministic responses thus was 2*(6 + 1 + 1 + 1) + 4*8 = 50, the first factor of 2 corresponding to inclusion of temporally differenced as well unmodified waveforms. The present regression strategy was accomplished in one step, which differs modestly from the previously described serial regression strategy (Fox et al., 2005).

Construction of Regions of Interest

ROI for functional connectivity analyses were determined from a meta-analysis of four previously published event-related fMRI studies of young adults performing the Posner task (Astafiev et al., 2003, 2004; Corbetta et al., 2000; Kincade et al., 2005). For each study, responses to the cue were identified by a whole-brain voxel-wise ANOVA using MR frame as factor. The resulting F score maps were converted to equally probable Z scores that were then combined using a fixed-effects analysis and the resulting map then subjected to automatic peak search. Peaks closer than 10 mm were consolidated by algebraically averaging their coordinates. ROI were defined around peaks by thresholding the map at thresholds chosen to yield regions of approximately constant volume. Eight ROIs were selected on the basis of a priori knowledge as representing the dorsal attention network (DAN). Five regions representing the ventral attention network (VAN)

were similarly defined on the basis of differential responses to the target following invalid versus valid cues (MR frame × cue validity interaction effect). All ROIs are listed in Table S1.

FC MRI Correlation Analysis

The first step in all FC analyses was to extract BOLD time courses from each ROI (defined as described above) by averaging over voxels within each region. To compute FC maps corresponding to a selected seed ROI, the regional time course was correlated against all other voxels within the brain as originally described by Biswal et al. (1995). The present main results (regional FC) were obtained by computing Pearson correlation coefficients (r) for region pairs. Statistical tests on regional FC results were computed after application of Fisher's z transform $(z = 0.5\ln((1 + r)/(1 - r)))$, which yields variates that are approximately normally distributed (Zar, 1996).

Diffusion Tractography Imaging (DTI)

DTI data was acquired on six subjects in 48 directions, 2.5 mm cubic resolution, b = 800 s/mm², with five averages and was analyzed similar to Shimony et al. (2006). The images were realigned across encodings and data sets to correct for electronic shift and head movement. Full-brain streamline tractography was performed on all subjects after placing starting seed points on 1 mm resolution grid. The SLF tracks were filtered by selecting tracks that passed through both a large region in the deep white matter of the posterior frontal lobe and through the deep white matter of the parietal lobe. The AF tracks were selected to pass through the same region in the posterior frontal and a region in the deep white matter of the temporal lobe. A consensus volume was created from the tracks in all six subjects, which was then surface rendered for display. For the probabilistic tracking, the data were analyzed using Bayesian probability theory (Behrens et al., 2003). The lesion spot in Figure 7B (red) was transformed to each subject's individual space and used as a seed region for probabilistic tracking. Probability in each voxel was normalized to the voxel with highest connectivity. These results were then transformed to atlas space and averaged across subjects. For display purposes, voxels with probabilities above 5% or 10% were colored with two shades of blue, and they follow the expected location of the SLF and AF.

REFERENCES

Arrington, C.M., Carr, T.H., Mayer, A.R., and Rao, S.M. (2000). Neural mechanisms of visual attention: object-based selection of a region in space. J. Cogn. Neurosci. *12*, 106–117.

Astafiev, S.V., Shulman, G.L., Stanley, C.M., Snyder, A.Z., Van Essen, D.C., and Corbetta, M. (2003). Functional organization of human intraparietal and frontal cortex for attending, looking, and pointing. J. Neurosci. *23*, 4689–4699.

Astafiev, S.V., Stanley, C.M., Shulman, G.L., and Corbetta, M. (2004). Extrastriate body area in human occipital cortex responds to the performance of motor actions. Nat. Neurosci. 7, 542–548.

Astafiev, S.V., Shulman, G.L., and Corbetta, M. (2006). Visuospatial reorienting signals in the human temporo-parietal junction are independent of response selection. Eur. J. Neurosci. 23, 591–596.

Bartolomeo, P., Thiebaut de Schotten, M., and Doricchi, F. (2007). Left unilateral neglect as a disconnection syndrome. Cereb. Cortex, in press. Published online January 31, 2007. 10.1093/cercor/bhl181.

Behrens, T.E., Woolrich, M.W., Jenkinson, M., Johansen-Berg, H., Nunes, R.G., Clare, S., Matthews, P.M., Brady, J.M., and Smith, S.M. (2003). Characterization and propagation of uncertainty in diffusion-weighted MR imaging. Magn. Reson. Med. 50, 1077–1088.

Biswal, B., Yetkin, F.Z., Haughton, V.M., and Hyde, J.S. (1995). Functional connectivity in the motor cortex of resting human brain using echo-planar MRI. Magn. Reson. Med. 34, 537–541.

Boynton, G.M., Engel, S.A., Glover, G.H., and Heeger, D.J. (1996). Linear systems analysis of functional magnetic resonance imaging in human VI. J. Neurosci. 16, 4207–4221.

Corbetta, M., and Shulman, G.L. (2002). Control of goal-directed and stimulus-driven attention in the brain. Nat. Rev. Neurosci. 3, 201–215.

Corbetta, M., Akbudak, E., Conturo, T.E., Snyder, A.Z., Ollinger, J.M., Drury, H.A., Linenweber, M.R., Petersen, S.E., Raichle, M.E., Van Essen, D.C., and Shulman, G.L. (1998). A common network of functional areas for attention and eye movements. Neuron 21, 761–773.

Corbetta, M., Kincade, J.M., Ollinger, J.M., McAvoy, M.P., and Shulman, G.L. (2000). Voluntary orienting is dissociated from target detection in human posterior parietal cortex. Nat. Neurosci. 3, 292–297.

Corbetta, M., Kincade, J.M., and Shulman, G.L. (2002). Neural systems for visual orienting and their relationships to spatial working memory. J. Cogn. Neurosci. 14, 508–523.

Corbetta, M., Kincade, M.J., Lewis, C., Snyder, A.Z., and Sapir, A. (2005). Neural basis and recovery of spatial attention deficits in spatial neglect. Nat. Neurosci. 8, 1603–1610.

Cordes, D., Haughton, V.M., Arfanakis, K., Carew, J.D., Turski, P.A., Moritz, C.H., Quigley, M.A., and Meyerand, M.E. (2001). Frequencies contributing to functional connectivity in the cerebral cortex in "resting-state" data. AJNR Am. J. Neuroradiol. 22, 1326–1333.

Diller, L., and Weinberg, J. (1977). Hemi-inattention in rehabilitation: the evolution of a rationale remediation program. In Hemi-Inattention and Hemisphere Specialization, E.A. Weinstein and R.P. Friedland, eds. (New York: Raven), pp. 63–82.

Downar, J., Crawley, A.P., Mikulis, D.J., and Davis, K.D. (2000). A multimodal cortical network for the detection of changes in the sensory environment. Nat. Neurosci. 3, 277–283.

Fox, M.D., Snyder, A.Z., Vincent, J.L., Corbetta, M., Van Essen, D.C., and Raichle, M.E. (2005). The human brain is intrinsically organized into dynamic, anticorrelated functional networks. Proc. Natl. Acad. Sci. USA 102, 9673–9678.

Fox, M.D., Corbetta, M., Snyder, A.Z., Vincent, J.L., and Raichle, M.E. (2006). Spontaneous neuronal activity distinguishes human dorsal and ventral attention systems. Proc. Natl. Acad. Sci. USA 103, 10046–10051.

Friedrich, F.J., Egly, R., Rafal, R.D., and Beck, D. (1998). Spatial attention deficits in humans: a comparison of superior parietal and temporal-parietal junction lesions. Neuropsychology 12, 193–207.

Gaffan, D., and Hornak, J. (1997). Visual neglect in the monkey. Representation and disconnection. Brain 120, 1647–1657.

Greicius, M.D., Krasnow, B., Reiss, A.L., and Menon, V. (2003). Functional connectivity in the resting brain: a network analysis of the default mode hypothesis. Proc. Natl. Acad. Sci. USA 100, 253–258.

Greicius, M.D., Srivastava, G., Reiss, A.L., and Menon, V. (2004). Default-mode network activity distinguishes Alzheimer's disease from

healthy aging: evidence from functional MRI. Proc. Natl. Acad. Sci. USA 101, 4637–4642.

Hampson, M., Peterson, B.S., Skudlarski, P., Gatenby, J.C., and Gore, J.C. (2002). Detection of functional connectivity using temporal correlations in MR images. Hum. Brain Mapp. 15, 247–262.

Hampson, M., Driesen, N.R., Skudlarski, P., Gore, J.C., and Constable, R.T. (2006a). Brain connectivity related to working memory performance. J. Neurosci. 26, 13338–13343.

Hampson, M., Tokoglu, F., Sun, Z., Schafer, R.J., Skudlarski, P., Gore, J.C., and Constable, R.T. (2006b). Connectivity-behavior analysis reveals that functional connectivity between left BA39 and Broca's area varies with reading ability. Neuroimage 31, 513–519.

Heilman, K.M., and Van Den Abell, T. (1980). Right hemisphere dominance for attention: the mechanism underlying hemispheric asymmetries of inattention (neglect). Neurology 30, 327–330.

Heilman, K.M., Watson, R.T., and Valenstein, E. (1985). Neglect and related disorders. In Clinical Neuropsychology, K.M. Heilman and E. Valenstein, eds. (New York: Oxford), pp. 243–293.

Hillis, A.E. (2006). Neurobiology of unilateral spatial neglect. Neuroscientist 12, 153–163.

Husain, M., and Kennard, C. (1996). Visual neglect associated with frontal lobe infarction. J. Neurol. 243, 652–657.

Husain, M., and Rorden, C. (2003). Non-spatially lateralized mechanisms in hemispatial neglect. Nat. Rev. Neurosci. 4, 26–36.

Karnath, H.O., Ferber, S., and Himmelbach, M. (2001). Spatial awareness is a function of the temporal not the posterior parietal lobe. Nature 411, 950–953.

Karnath, H.O., Himmelbach, M., and Rorden, C. (2002). The subcortical anatomy of human spatial neglect: putamen, caudate nucleus and pulvinar. Brain 125, 350–360.

Karnath, H.O., Fruhmann Berger, M., Kuker, W., and Rorden, C. (2004). The anatomy of spatial neglect based on voxelwise statistical analysis: a study of 140 patients. Cereb. Cortex 14, 1164–1172.

Kastner, S., and Ungerleider, L.G. (2000). Mechanisms of visual attention in the human cortex. Annu. Rev. Neurosci. 23, 315–341.

Kincade, J.M., Abrams, R.A., Astafiev, S.V., Shulman, G.L., and Corbetta, M. (2005). An event-related functional magnetic resonance imaging study of voluntary and stimulus-driven orienting of attention. J. Neurosci. 25, 4593–4604.

Laufs, H., Krakow, K., Sterzer, P., Eger, E., Beyerle, A., Salek-Haddadi, A., and Kleinschmidt, A. (2003). Electroencephalographic signatures of attentional and cognitive default modes in spontaneous brain activity fluctuations at rest. Proc. Natl. Acad. Sci. USA 100, 11053–11058.

Lowe, M.J., Phillips, M.D., Lurito, J.T., Mattson, D., Dzemidzic, M., and Mathews, V.P. (2002). Multiple sclerosis: low-frequency temporal blood oxygen level-dependent fluctuations indicate reduced functional connectivity initial results. Radiology 224, 184–192.

Macaluso, E., Frith, C.D., and Driver, J. (2002). Supramodal effects of covert spatial orienting triggered by visual or tactile events. J. Cogn. Neurosci. 14, 389–401.

Malhotra, P., Coulthard, E., and Husain, M. (2006a). Hemispatial neglect, balance and eye-movement control. Curr. Opin. Neurol. 19, 14–20.

Malhotra, P.A., Parton, A.D., Greenwood, R., and Husain, M. (2006b). Noradrenergic modulation of space exploration in visual neglect. Ann. Neurol. 59, 186–190.

Mesulam, M.M. (1999). Spatial attention and neglect: parietal, frontal and cingulate contributions to the mental representation and attentional targeting of salient extrapersonal events. Philos. Trans. R. Soc. Lond. B Biol. Sci. 354, 1325–1346.

Milner, A.D., and McIntosh, R.D. (2005). The neurological basis of visual neglect. Curr. Opin. Neurol. 18, 748–753.

Morrow, L.A., and Ratcliff, G. (1988). The disengagement of covert attention and the neglect syndrome. Psychobiology 16, 261–269.

Mort, D.J., Malhotra, P., Mannan, S.K., Rorden, C., Pambakian, A., Kennard, C., and Husain, M. (2003). The anatomy of visual neglect. Brain 126, 1986–1997.

Pardo, J.V., Fox, P.T., and Raichle, M.E. (1991). Localization of a human system for sustained attention by positron emission tomography. Nature 349, 61–64.

Peers, P.V., Ludwig, C.J., Rorden, C., Cusack, R., Bonfiglioli, C., Bundesen, C., Driver, J., Antoun, N., and Duncan, J. (2005). Attentional functions of parietal and frontal cortex. Cereb. Cortex 15, 1469–1484.

Petrides, M., and Pandya, D.N. (2002). Association pathways of the prefrontal cortex and functional observations. In Principles of Frontal Lobe Function, D.T. Stuss and R.T. Knight, eds. (New York: Oxford University Press), pp. 31–50.

Posner, M.I., Walker, J.A., Friedrich, F.J., and Rafal, R.D. (1984). Effects of parietal injury on covert orienting of attention. J. Neurosci. 4, 1863–1874.

Quigley, M., Cordes, D., Wendt, G., Turski, P., Moritz, C., Haughton, V., and Meyerand, M.E. (2001). Effect of focal and nonfocal cerebral lesions on functional connectivity studied with MR imaging. AJNR Am. J. Neuroradiol. 22, 294–300.

Quigley, M., Cordes, D., Turski, P., Moritz, C., Haughton, V., Seth, R., and Meyerand, M.E. (2003). Role of the corpus callosum in functional connectivity. AJNR Am. J. Neuroradiol. 24, 208–212.

Robertson, I.H. (2001). Do we need the "lateral" in unilateral neglect? Spatially nonselective attention deficits in unilateral neglect and their implications for rehabilitation. Neuroimage 14, S85–S90.

Robertson, I.H., Tegner, R., Tham, K., Lo, A., and Nimmo-Smith, I. (1995). Sustained attention training for unilateral neglect: theoretical and rehabilitation implications. J. Clin. Exp. Neuropsychol. 17, 416–430.

Robertson, I.H., Mattingley, J.B., Rorden, C., and Driver, J. (1998). Phasic alerting of neglect patients overcomes their spatial deficit in visual awareness. Nature 395, 169–172.

Rueckert, L., and Grafman, J. (1996). Sustained attention deficits in patients with right frontal lesions. Neuropsychologia 34, 953–963.

Schluppeck, D., Glimcher, P., and Heeger, D.J. (2005). Topographic organization for delayed saccades in human posterior parietal cortex. J. Neurophysiol. 94, 1372–1384.

Schmahmann, J.D., and Pandya, D.N. (2006). Fiber Pathways of the Brain (New York: Oxford University Press).

Serences, J.T., Yantis, S., Culberson, A., and Awh, E. (2004). Preparatory activity in visual cortex indexes distractor suppression during covert spatial orienting. J. Neurophysiol. 92, 3538–3545.

Sereno, M.I., Pitzalis, S., and Martinez, A. (2001). Mapping of contralateral space in retinotopic coordinates by a parietal cortical area in humans. Science 294, 1350–1354.

Shapiro, K., Hillstrom, A.P., and Husain, M. (2002). Control of visuotemporal attention by inferior parietal and superior temporal cortex. Curr. Biol. 12, 1320–1325.

Shimony, J.S., Burton, H., Epstein, A.A., McLaren, D.G., Sun, S.W., and Snyder, A.Z. (2006). Diffusion tensor imaging reveals white matter reorganization in early blind humans. Cereb. Cortex 16, 1653–1661.

Silver, M.A., Ress, D., and Heeger, D.J. (2005). Topographic maps of visual spatial attention in human parietal cortex. J. Neurophysiol. 94, 1358–1371.

Talairach, J., and Tournoux, P. (1988). Co-Planar Stereotaxic Atlas of the Human Brain (New York: Thieme Medical Publishers, Inc.).

Thiebaut de Schotten, M., Urbanski, M., Duffau, H., Volle, E., Levy, R., Dubois, B., and Bartolomeo, P. (2005). Direct evidence for a parietal-frontal pathway subserving spatial awareness in humans. Science 309, 2226–2228.

Vallar, G., and Perani, D. (1987). The anatomy of spatial neglect in humans. In Neurophysiological and Neuropsychological Aspects of Spatial Neglect, M. Jeannerod, ed. (Amsterdam: Elsevier Science Publishers), pp. 235–258.

Vincent, J.L., Snyder, A.Z., Fox, M.D., Shannon, B.J., Andrews, J.R., Raichle, M.E., and Buckner, R.L. (2006). Coherent spontaneous activity identifies a hippocampal-parietal memory network. J. Neurophysiol. 96, 3517–3531.

Waites, A.B., Briellmann, R.S., Saling, M.M., Abbott, D.F., and Jackson, G.D. (2006). Functional connectivity networks are disrupted in left temporal lobe epilepsy. Ann. Neurol. 59, 335–343.

Whalley, H.C., Simonotto, E., Marshall, I., Owens, D.G., Goddard, N.H., Johnstone, E.C., and Lawrie, S.M. (2005). Functional disconnectivity in subjects at high genetic risk of schizophrenia. Brain 128, 2097–2108.

Wilkins, A.J., Shallice, T., and McCarthy, R. (1987). Frontal lesions and sustained attention. Neuropsychologia 25, 359–365.

Zar, J.H. (1996). Biostatistical Analysis, Third Edition (Upper Saddle River, NJ: Prentice-Hall, Inc.).